



Using ultrafast infrared multidimensional correlation spectroscopy to aid in vibrational spectral peak assignments

John B. Asbury, Tobias Steinel, M.D. Fayer^{*}

Department of Chemistry, Stanford University, Stanford, CA 94305, USA

Received 5 June 2003; in final form 11 September 2003

Published online: 20 October 2003

Abstract

Ultrafast infrared heterodyne detected vibrational stimulated echoes with full phase information are used to obtain the vibrational correlation spectrum from a mixture of metal-carbonyl compounds. The linear absorption spectrum displays four peaks in the carbonyl stretching region. In the absence of knowledge of the molecules that make up the mixture, the absorption spectrum could arise from four molecules that each produces a single peak to one molecule with four peaks. In contrast, the correlation spectrum displays four peaks on the diagonal and off-diagonal peaks that make it straightforward to determine which peaks belong to a particular molecule.

© 2003 Elsevier B.V. All rights reserved.

1. Introduction

Vibrational spectroscopy is widely used to determine the identity and structure of molecules. The mid-IR region of the spectrum is called the ‘finger print’ region because of the characteristic absorption features that can be assigned to various functional groups of molecules. However, the use of IR vibrational spectroscopy to identify compounds becomes much more difficult when there is an unknown mixture of compounds. From a spectrum that has multiple peaks in a spectral re-

gion associated with a particular functional group, it cannot be readily determined whether the peaks belong to one molecule or a number of different molecules. This is an important and complex problem in analytical chemistry that often arises. Examples include studying the species in a reaction mixture of short-lived intermediates, or identifying multiple metal centers in proteins to study their function and dynamics [1]. It is also desirable to have a method that can enhance a vibrational spectrum with sufficient time resolution to study short-lived intermediates.

Recently, ultrafast vibrational echo experiments [2–5] have been expanded to multidimensional methods [6–16]. In this Letter, a simple illustration is provided of the use of ultrafast infrared

^{*} Corresponding author. Fax: +1 650 723 4817.

E-mail address: fayer@stanford.edu (M.D. Fayer).

stimulated vibrational echo correlation spectroscopy to aid in assigning vibrational peaks in a mixture of molecules that has a linear vibrational absorption spectrum that does not provide enough information to determine the number of molecules in the mixture or to associate peaks with a particular molecules.

The multidimensional stimulated vibrational echo technique measures the population and vibrational dephasing dynamics in two frequency dimensions, ω_τ and ω_m . The ω_τ axis in a two-dimensional correlation spectrum displays the frequency of the first interaction of the sample with the radiation field (first IR pulse in the three pulse sequence). The ω_m axis displays the frequency at which the vibrational echo is emitted following the third interaction with the radiation field (third IR pulse). The position of peaks in the two-dimensional frequency plane are described by their coordinates, (ω_m, ω_τ) . Peaks in a linear absorption spectrum will appear as peaks along the diagonal in the vibrational echo correlation spectrum, that is where $\omega_m = \omega_\tau$. However, in a correlation spectrum, vibrations that are coupled through the anharmonic molecular potential will have off-diagonal peaks ‘coherence transfer’ peaks where $\omega_m \neq \omega_\tau$ [17]. For two coupled modes of a molecule with frequencies ω_a and ω_b , the diagonal peaks are at (ω_a, ω_a) and (ω_b, ω_b) . With the splitting between the two lines, $\Delta = \omega_b - \omega_a$, the coordinates of the coherence transfer peaks are $(\omega_a, \omega_a + \Delta)$ and $(\omega_b, \omega_b - \Delta)$. The off-diagonal coherence transfer peaks in the correlation spectrum show which peaks in the absorption spectrum are coupled and, therefore, which transitions are on the same molecule.

Fig. 1 is an IR absorption spectrum of the carbonyl stretch region for metal carbonyls. The spectrum shows four well-resolved peaks. From this spectrum alone, it is not possible to determine if there is one molecule with four peaks or as many as four molecule each with one peak. If there is more than one molecule, it is not possible to tell which peaks belong to the same molecule. As shown below, from the correlation spectrum it is straightforward to determine which peaks belong to the same molecule by the coherence transfer peaks discussed above. In addition to the off-

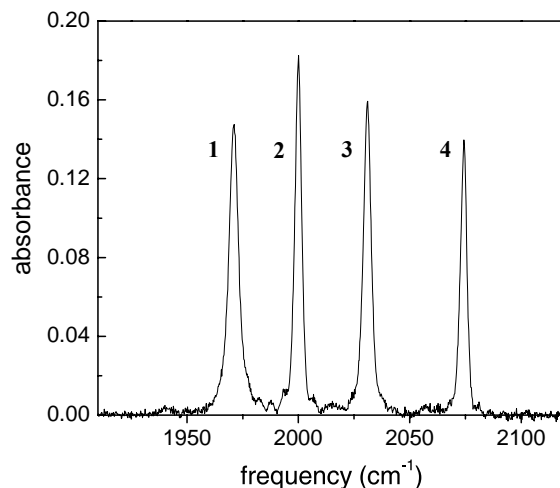


Fig. 1. The sample's IR absorption spectrum of the carbonyl stretch region for metal carbonyls. The spectrum shows four well-resolved peaks. From this spectrum alone, it is not possible to determine if there is one molecule with four peaks or as many as four molecule each with one peak.

diagonal coherence transfer peaks, there are also off-diagonal peaks for the 1–2 transitions of each mode shifted by the mode vibrational anharmonicity. Furthermore, there are off-diagonal peaks shifted by the combination band shift for coupled modes. However, in the correlation spectrum the diagonal peaks and the off-diagonal coherence transfer peaks are positive going, but the anharmonicity peaks and the combination band peaks are negative going. Therefore, it is straightforward to determine the relevant peaks in the spectrum.

2. Experimental procedures

The ultrashort IR pulses used for the experiments were generated using a Ti:sapphire regeneratively amplified laser/OPA system. The output of the regen is 26 fs transform limited 2/3 mJ pulses at 1 kHz rep rate. These are used to pump a substantially modified Spectra Physics short pulse IR OPA. The output of the OPA is compressed to produce <50 fs virtually transform limited IR pulses as measured by collinear autocorrelation. For the experiments, the compression was readjusted to give transform limited pulses in the

sample as measured by a sample that gave a purely non-resonant signal.

For the heterodyne detected multidimensional stimulated vibrational echoes, the IR beam is split into five beams. Three of the beams are the excitation beams for the stimulated vibrational echo. A fourth beam is the local oscillator (LO) used to heterodyne detect the vibrational echo signal [9–11,18]. All of the beams that pass through the sample are optically identical and are compensated for GVD simultaneously. The vibrational echo signal combined with the LO is passed through a monochromator. For the spectrally resolved pump–probe experiments, one of the excitation beams is used for pump–probe experiments. The fifth beam is 10 times weaker than the others and is used as the probe beam. After passing through the sample, the probe beam is directed into the monochromator. Depending on the experiment, the heterodyne detected echo or the probe beam is detected by a 32 element MCT array. At each monochromator setting, the array detects 32 individual wavelengths. The data were processed using a computer that acted as a digital lock-in amplifier that was synchronized to an optical chopper. For the spectrally resolved pump–probe experiments, the change in transmission spectrum was collected as a function of the delay between the pump and probe pulses. More details of the experiment are given elsewhere [12].

The sample, (acetylacetonato)dicarbonylIridium ($\text{Ir}(\text{CO})_2(\text{acac})$) and (cyclopentadienyl)dicarbonylCobalt ($\text{Co}(\text{CO})_2\text{Cp}$), in 2 mM solution in hexane, was held in a sample cell of CaF_2 flats with a spacing of 100 μm . The peak absorbance of the samples was ~ 0.18 (see Fig. 1). Such a low absorbance is necessary to prevent serious distortions of the pulses as they propagate through the sample.

The phase-resolved, heterodyne detected, stimulated vibrational echoes were measured as a function of one frequency variable, ω_m , and two time variables, τ and T_w , which are defined as the time between the first and second radiation field-matter interactions and the second and third interactions, respectively [9–11,18]. The measured signal is the absolute value squared of the sum of the vibrational echo signal electric field, S , and the

local oscillator electric field, L : $|L + S|^2 = L^2 + 2LS + S^2$. The L^2 term is time-independent and the S^2 is negligibly small; hence, neither contributes to the time dependence of the signal. The spectrum of the $2LS$ term is displayed along the ω_m frequency axis. As the τ variable is scanned in 2 fs steps, the phase of S is scanned relative to the fixed L , resulting in an interferogram measured as a function of the τ variable. The interferogram contains the amplitude, sign, frequency, and phase of the vibrational echo electric field as it varies with τ . By Fourier transformation, this interferogram is converted into the frequency variable ω_τ . In NMR, the ω_τ and the ω_m axes are generally referred to as the ω_1 and the ω_3 axes, respectively [17].

The interferogram contains both the absorptive and dispersive components of the vibrational echo signal. However, two sets of quantum pathways can be measured independently by appropriate time ordering of the pulses in the experiment [9,10,18]. With pulses 1 and 2 at the time origin, pathway 1 or 2 is obtained by scanning pulse 1 or 2 to negative time, respectively. By adding the Fourier transforms of the interferograms from the two pathways, the dispersive component cancels leaving only the absorptive component. The 2D vibrational echo correlation spectra are constructed by plotting the amplitude of the absorptive part of the stimulated vibrational echo as a function of both ω_m and ω_τ .

Lack of perfect knowledge of the timing of the pulses and consideration of chirp on the vibrational echo pulse requires a ‘phasing’ procedure to be used. The projection slice theorem [9,10,17,18] is employed to generate the absorptive 2D correlation spectrum. The projection of the absorptive 2D correlation spectrum onto the ω_m axis is equivalent to the IR pump–probe spectrum recorded at the same T_w , as long as all the contributions to the stimulated vibrational echo are absorptive. Consequently, comparison of the projected 2D stimulated vibrational echo spectrum with the pump–probe spectrum permits the correct isolation of the absorptive vibrational echo correlation spectrum from the 2D spectrum obtained from the addition of the two quantum pathways.

The frequency dependent phasing factor used to correct the 2D spectra has the form [11,12]

$$S_C(\omega_m, \omega_\tau) = S_1(\omega_m, \omega_\tau)\Phi_1(\omega_m, \omega_\tau) + S_2(\omega_m, \omega_\tau)\Phi_2(\omega_m, \omega_\tau)$$

$$\Phi_1(\omega_m, \omega_\tau) = \exp [i[\omega_m\Delta\tau_{LO,E} + \omega_\tau\Delta\tau_{1,2} + Q\omega_m\omega_m + C\omega_m\omega_\tau]]$$

$$\Phi_2(\omega_m, \omega_\tau) = \exp [i(\omega_m\Delta\tau_{LO,E} - \omega_\tau\Delta\tau_{1,2} + Q\omega_m\omega_m + C\omega_m\omega_\tau)] \quad (1)$$

Each term in Eq. (1) has a well-defined physical origin. S_C is the correlation spectrum. S_1 and S_2 are the spectra recorded for pathways 1 and 2, respectively. $\Delta\tau_{LO,E}$ accounts for the lack of perfect knowledge of the time separation of the LO pulse and the vibrational echo pulse; the term involving Q accounts for linear chirp introduced into the echo pulse by the rear window of the sample cell; $\Delta\tau_{1,2}$ accounts for the lack of perfect knowledge of the time origins of excitation pulses 1 and 2; and the term involving C accounts for the linear chirp caused by propagation of the echo pulse through sample. Fig. 2 compares the projection of the vibrational echo correlation spectrum with the pump-probe spectrum at the completion of the phasing procedure. The projection and the pump-probe spectrum are quite similar. For the purposes of the peak assignment discussed here, the phasing

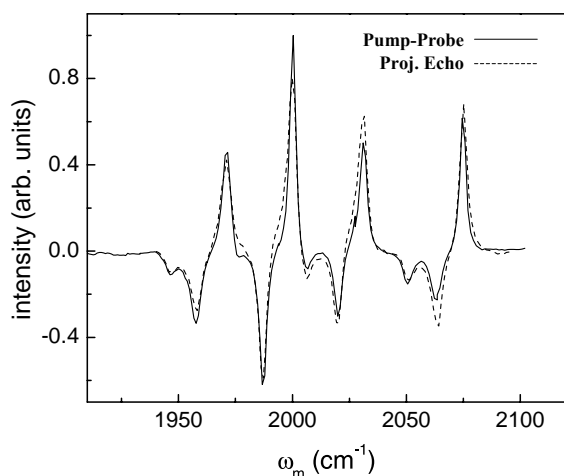


Fig. 2. Comparison of the projected vibrational echo correlation spectrum onto the ω_m axis with the pump-probe spectrum following the phasing procedure.

is adequate. The origin of the differences between the two spectra will be discussed below.

3. Results and discussion

Fig. 3 displays the correlation spectrum taken with the separation between the second and third pulses, $T_w = 400$ fs. The correlation spectrum has 16 peaks, eight positive going peaks (labeled with +) and eight negative going peaks (labeled with -). Each contour represents a 10% change in amplitude. The molecules studied in this work are completely analogous to (acetylacetonato)dicarbonylrhodium(I) ($\text{Rh}(\text{CO})_2(\text{acac})$). The metal carbonyl, $\text{Rh}(\text{CO})_2\text{acac}$ has been studied in great detail using vibrational echo techniques [7–10,19–24]. All of the features can be assigned in the correlation spectrum using diagrammatic perturbation theory [9,10,22,23,25]. For a mixture of metal carbonyls, the same basic structure will hold, as it will for any molecule with coupled vibrations if the experiment is conducted with IR pulses of

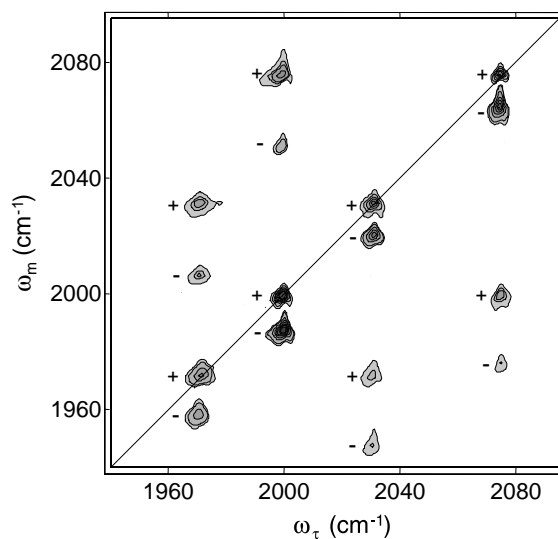


Fig. 3. Ultrafast infrared vibrational correlation spectrum of the same sample that gave the linear absorption spectrum in Fig. 1. The correlation spectrum has 16 peaks, eight positive going peaks (labeled with +) and eight negative going peaks (labeled with -). Each contour represents a 10% change in amplitude.

sufficient bandwidth to span all of the relevant features.

The positive going peaks on the diagonal are the peaks in the absorption spectrum. ω_τ is the frequency of the first interaction. ω_m is the frequency of the vibrational echo emission. The first interaction with the radiation field is at the absorption frequency of one of the modes (peaks in the linear spectrum) and produces a ‘coherence’ between the ground state, 0, and the first excited state, 1. A ‘coherence’ reflects the generation of a coherent superposition state, in this case between the 0 and 1 states. The equivalent of a coherence in NMR is an in plane processing magnetization [17]. The second interaction produces a population either in 1 or 0, and the third interaction produces a 0–1 coherence, which gives rise to emission of the vibrational echo at the 0–1 transition frequency. Only the ground state and first excited state, 0 and 1 of the given mode are involved. In the same manner, each mode in the spectrum will give rise to a diagonal peak. All of the other peaks are off-diagonal and involve more than two states either of one mode or two states belonging to two different modes of a molecule.

The negative going peak immediately below each diagonal peak is shifted from the diagonal peak by the vibrational anharmonicity of the mode. The first interaction with the radiation field produces a coherence between the 0 and 1 states. The second interaction produces a population in the 1 state. The third interaction produces a coherence between the 1 and 2 states, which gives rise to vibrational echo emission at the 1–2 transition frequency. Because the first interaction is at the 0–1 frequency and the emission is at the 1–2 transition frequency, the ‘anharmonic peak’ is off-diagonal and shifted along the ω_m axis by the difference in the 0–1 and 1–2 transition frequencies, the mode’s anharmonicity.

Moving along the ω_τ axis either to the right or to the left of each diagonal peak, another positive going peak is found. In NMR these are called ‘coherence transfer’ peaks [17]. Such peaks will only occur if the transition that gives rise to the diagonal peak is coupled to the transition of another mode. For two, modes a and b , with frequencies ω_a and ω_b , the diagonal peaks are at (ω_a, ω_a) and

(ω_b, ω_b) . With the splitting between the two lines $\Delta = \omega_b - \omega_a$, the coordinates (ω_m, ω_τ) of the off-diagonal peaks are $(\omega_a, \omega_a + \Delta)$ and $(\omega_b, \omega_b - \Delta)$. The radiation field/system pathway that gives rise to such an off-diagonal peak is as follows. The first interaction at ω_a produces a 0–1 coherence on a . The second interaction at ω_a produces a population in the *ground state* on a , and the third interaction at ω_b produces a 0–1 coherence on b , which gives rise to vibrational echo emission at ω_b .

Directly below each coherence transfer peak is a negative going peak. These arise from combination band transitions. The splitting between the positive going coherence transfer peak and the negative going combination band peak along the ω_m axis is the combination band shift. The combination band shift peaks come about in the following manner. Starting with mode a , the first interaction at ω_a produces a 0–1 coherence on a . The second interaction at ω_a produces a population in the *excited state* on a , and the third interaction at $\omega_b - \delta$ produces a coherence on b , which gives rise to vibrational echo emission at the transition frequency $\omega_b - \delta$, where δ is the combination band shift.

There are 16 peaks in the correlation spectrum, eight are positive going (diagonal peaks and coherence transfer peaks) and eight are negative going (anharmonic peaks and combination band peaks). The vibrational echo emission is a fourth interaction with the radiation field. It is always at the coherence frequency generated by the third radiation field interaction. The coherence always involves a superposition state of an upper energy level β and a lower energy level α . The echo emission leaves the system in the lower level α of the superposition state. The positive going peaks have all modes in their *ground state* following vibrational echo emission. The negative going peaks leave one mode in a vibrational *excited state* after echo emission. In terms of linear spectroscopy, the negative going peaks would be associated with excited state transitions. The anharmonic shift can be observed if level 1 is populated and then the 1–2 transition is measured. The combination band shift can be measured if first level 1 is populated of one mode, and then the absorption of another mode is measured. Such transitions do not appear

in the ground state absorption spectrum. Therefore, it is the positive going peaks that aid in understanding the ground state absorption spectrum shown in Fig. 1.

Fig. 4 displays the correlation spectrum with only the positive going peaks shown. The peaks are labeled 1–4. Each contour represents a 10% change in amplitude. The lines connecting the off-diagonal coherence transfer peaks and the diagonal peaks are aids to the eye. Modes on the same molecule can be coupled through the anharmonic molecular potential. The coherence transfer peaks connect modes, represented by peaks on the diagonal that are coupled. From the correlation spectrum shown in Fig. 4, it is clear that peaks 1 and 3 are coupled and peaks 2 and 4 are coupled. In the linear spectrum displayed in Fig. 1, peaks 1 and 3 belong to the same molecule, and peaks 2 and 4 belong to the same molecule. The splitting between the peaks that belong to the same molecule is now known. As indicated in Fig. 4, peaks 1 and 3 belong to $\text{Co}(\text{CO})_2\text{Cp}$; they are the anti-

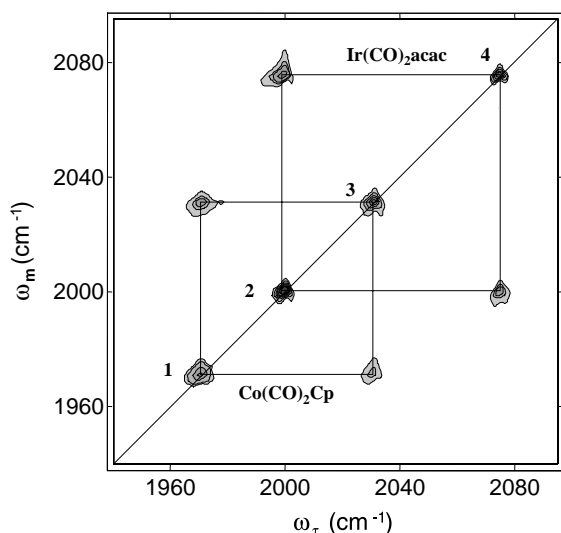


Fig. 4. The correlation spectrum with only the positive going peaks shown. Each contour represents a 10% change in amplitude. The off-diagonal coherence transfer peaks show which diagonal peaks are coupled. The lines are aids to the eye. It is clear that peaks 1 and 3 are coupled and peaks 2 and 4 are coupled. In the linear spectrum Fig. 1, peaks 1 and 3 belong to the same molecule and peaks 2 and 4 belong to the same molecule.

symmetric and symmetric stretches of $\text{Co}(\text{CO})_2\text{Cp}$, respectively. Peaks 2 and 4 are the antisymmetric and symmetric stretches of $\text{Ir}(\text{CO})_2(\text{acac})$, respectively. While the correlation spectrum cannot determine the identity of the molecule that belongs to the peaks, it significantly extends the information that can be obtained from the linear absorption spectrum. In addition to determining which peaks are coupled, the anharmonicities of the modes and the combination band shifts are determined. These are listed in Table 1.

The method demonstrated above is based strictly on the positions of the peaks in the two-dimensional plane (see Figs. 3 and 4). In addition, the shapes of the peaks can provide information on vibrational dephasing dynamics, which describe the time evolution of the system [9,10]. Selection of the purely absorptive component of vibrational echo correlation spectra can simplify congested spectra and improve resolution. Purely absorptive vibrational echo correlation spectra have been presented for the $\text{Rh}(\text{CO})_2(\text{acac})$ model system in hexane solution [9,10] and have been obtained recently for the hydroxyl stretch of methanol [11–13] and water [14,15].

Obtaining purely absorptive features in a correlation spectrum requires selecting the appropriate phase from the numerical Fourier transform of the time domain data. When there are multiple peaks in the spectrum, it is necessary for the time separation between the local oscillator pulse and the portion of the vibrational echo pulse generated by each transition to be the same for all transi-

Table 1
Anharmonic and combination shifts

	Anharmonic shift ^a (cm ⁻¹)	Combination band shift ^b (cm ⁻¹)
$\text{Ir}(\text{CO})_2(\text{acac})$ antisymmetric stretch	12.2	24.3
$\text{Ir}(\text{CO})_2(\text{acac})$ symmetric stretch	11.6	24.3
$\text{Co}(\text{CO})_2\text{Cp}$ antisymmetric stretch	14.0	24.7
$\text{Co}(\text{CO})_2\text{Cp}$ symmetric stretch	11.3	24.7

^a Estimated error: ± 0.3 cm⁻¹.

^b Estimated error: ± 0.5 cm⁻¹.

tions. For transitions having very similar linear line widths, as in the case of the $\text{Rh}(\text{CO})_2(\text{acac})$ [9,10], the time separations between the local oscillator pulse and the vibrational echo pulses emitted from all transitions are nearly the same. As a result, the phase to obtain purely absorptive features for the transitions can be set simultaneously [9,10]. However, in the case of the mixture of $\text{Ir}(\text{CO})_2(\text{acac})$ and $\text{Co}(\text{CO})_2\text{Cp}$ presented here, the two molecules have significantly different linear line widths, differing by a factor >2 across the spectrum (see Fig. 1). As a result, the features in the vibrational echo correlation spectra displayed in Figs. 3 and 4 are not purely absorptive, producing some distortions in the peak shapes. The non-purely absorptive peak shapes cause the differences in the pump–probe data and the projection of the vibrational echo data onto the ω_m axis seen in Fig. 2.

The time separations between the local oscillator pulse and the vibrational echo pulses emitted from the transitions differ because the free-induction decays (FIDs) of the transitions are different. Consequently, the phase necessary to obtain purely absorptive features cannot be simultaneously set for the entire spectrum. One way to overcome this problem is to use a monochromator resolution that is very high. If the inverse of the resolution is much greater than the FID times for all transitions, the effective FID times are the inverse of the resolution. The disadvantage of very high resolution is that it decreases the spectral bandwidth that can be detected in a single measurement with the array detector. We are currently developing a new phasing procedure that allows the appropriate phase to be independently set for each transition in the vibrational echo correlation spectrum without the necessity of using very high spectral resolution.

4. Concluding remarks

This report demonstrates the usefulness of vibrational echo correlation spectroscopy for assigning the vibrational spectra of complex mixtures. Some caution must be exercised in interpreting the correlation spectrum. While it is

clear which peaks are coupled, and therefore on the same molecule, it is not safe to say that peaks that are not coupled are on different molecules. For example, if a long alkyl chain connected the two molecules used in these experiments, the spectra, both the linear absorption spectrum and the correlation spectrum, would be virtually identical. Furthermore, spatially well-separated metal centers in a large protein would not be coupled. For several multiple metal centers in the same protein [1], it may be possible to identify which peaks in the absorption spectrum belong to the same center. The approach demonstrated here might become an important tool for the assignment of peaks in vibrational spectroscopy. The ultrafast nature of the measurement can be useful in examining short-lived transient species.

Acknowledgements

This work was supported by the Air Force Office of Scientific Research (Grant # F49620-01-1-0018) and the National Institutes of Health (1R01-GM61137). TS thanks the Emmy Noether program of the DFG for partial support.

References

- [1] T.I. Doukov, T.M. Iverson, J. Seravalli, S.W. Ragsdale, C.L. Drennan, *Science* 298 (2002) 567.
- [2] D. Zimdars, A. Tokmakoff, S. Chen, S.R. Greenfield, M.D. Fayer, T.I. Smith, H.A. Schwettman, *Phys. Rev. Lett.* 70 (1993) 2718.
- [3] A. Tokmakoff, M.D. Fayer, *J. Chem. Phys.* 102 (1995) 2810.
- [4] K.D. Rector, J.R. Engholm, C.W. Rella, J.R. Hill, D.D. Dlott, M.D. Fayer, *J. Phys. Chem. A* 103 (1999) 2381.
- [5] P. Hamm, M. Lim, R.M. Hochstrasser, *Phys. Rev. Lett.* 81 (1998) 5326.
- [6] M.T. Zanni, M.C. Asplund, R.M. Hochstrasser, *J. Chem. Phys.* 114 (2001) 4579.
- [7] K.A. Merchant, D.E. Thompson, M.D. Fayer, *Phys. Rev. Lett.* 86 (2001) 3899.
- [8] O. Golonzka, M. Khalil, N. Demirdöven, A. Tokmakoff, *Phys. Rev. Lett.* 86 (2001) 2154.
- [9] M. Khalil, N. Demirdöven, A. Tokmakoff, *J. Phys. Chem. A* 107 (2003) 5258.
- [10] M. Khalil, N. Demirdöven, A. Tokmakoff, *Phys. Rev. Lett.* 90 (2003) 047401.

- [11] J.B. Asbury, T. Steinel, C. Stromberg, K.J. Gaffney, I.R. Piletic, A. Goun, M.D. Fayer, *Chem. Phys. Lett.* 374 (2003) 362.
- [12] J.B. Asbury, T. Steinel, C. Stromberg, K.J. Gaffney, I.R. Piletic, M.D. Fayer, *J. Chem. Phys.*, accepted for publication.
- [13] J.B. Asbury, T. Steinel, C. Stromberg, K.J. Gaffney, I.R. Piletic, M.D. Fayer, *J. Phys. Chem. A*, submitted for publication.
- [14] J.B. Asbury, T. Steinel, C. Stromberg, S.A. Corcelli, C.P. Lawrence, J.L. Skinner, M.D. Fayer, *J. Phys. Chem. A*, submitted for publication.
- [15] T. Steinel, J.B. Asbury, S.A. Corcelli, C.P. Lawrence, J.L. Skinner, M.D. Fayer, *Science*, submitted.
- [16] S. Mukamel, *Ann. Rev. Phys. Chem.* 51 (2000) 691.
- [17] R.R. Ernst, G. Bodenhausen, A. Wokaun, *Nuclear Magnetic Resonance in One and Two Dimensions*, Oxford University Press, Oxford, 1987.
- [18] D.M. Jonas, *Annu. Rev. Phys. Chem.* 54 (2003) 425.
- [19] K.D. Rector, M.D. Fayer, *J. Chem. Phys.* 108 (1998) 1794.
- [20] M. Khalil, A. Tokmakoff, *Chem. Phys.* 266 (2001) 213.
- [21] N. Demirdoven, M. Khalil, O. Golonzka, A. Tokmakoff, *J. Phys. Chem. A* 105 (2001) 8030.
- [22] O. Golonzka, M. Khalil, N. Demirdoven, A. Tokmakoff, *J. Chem. Phys.* 115 (2001) 10814.
- [23] O. Golonzka, A. Tokmakoff, *J. Chem. Phys.* 115 (2001) 297.
- [24] D.E. Thompson, K.A. Merchant, M.D. Fayer, *J. Chem. Phys.* 115 (2001) 317.
- [25] S. Mukamel, *Principles of Nonlinear Optical Spectroscopy*, Oxford University Press, New York, 1995.